Spectroscopic Characterization of Recombinant Pea Cytosolic Ascorbate Peroxidase: Similarities and Differences with Cytochrome *c* Peroxidase[†]

Mikkel Nissum,[‡] Francesca Neri,[§] David Mandelman,[||] Thomas L. Poulos,[||] and Giulietta Smulevich*[,§]

Department of Chemistry, Odense University, Campusvej 55, DK-5230 Odense, Denmark, Department of Molecular Biology and Biochemistry, University of California at Irvine, Irvine, California 92617-3900, and Dipartimento di Chimica, Universita' di Firenze, Via G. Capponi 9, I-50121 Firenze, Italy

Received January 15, 1998; Revised Manuscript Received March 19, 1998

ABSTRACT: Recombinant pea cytosolic ascorbate peroxidase (APX) has been characterized by resonance Raman (RR) and electronic absorption spectroscopies. The ferric and ferrous forms together with the complexes with fluoride and imidazole have been studied and compared with the corresponding spectra of cytochrome *c* peroxidase (CCP). Ferric APX at neutral pH is a mixture of 6- and 5-coordinate high-spin and 6-c low-spin hemes, the latter two species being dominant. The results suggest that the low-spin form derives from a water/hydroxo ligand bound to the heme iron and not from a strong internal ligand as observed in CCP at alkaline pH. Two Fe−Im stretching modes are identified, as in CCP, but the RR frequencies confirm a weaker His163−Asp208 hydrogen bond than in CCP, as suggested on the basis of the X-ray structure [Patterson, W. R., and Poulos, T. L. (1995) *Biochemistry 34*, 4331−4341]. The data show that CCP and APX have markedly different orientations of the vinyl substituents on the heme chromophore resulting from different steric constraints exerted by the protein matrix.

Intra- and extracellular heme containing peroxidases are evolutionary related and constitute the "plant peroxidase superfamily". On the basis of sequence alignment, three well-separated classes can be distinguished within this superfamily. Class I includes the intracellular peroxidases of prokaryotic origin, class II the secretory fungal peroxidases, and class III the classical secretory plant peroxidases (*1*). Cytosolic ascorbate peroxidase (APX)[1] from pea (*Pisum sativum L.)* has 33% amino acid sequence identity with cytochrome *c* peroxidase (CCP) and belongs to class I (*2*, *3*). It functions by scavenging hydrogen peroxide and preferentially oxidizing ascorbate in this process. The functional enzyme is a noncovalently linked homodimer which is composed of two identical subunits (*4*).

APX has been expressed in large amounts in *Escherichia coli* (*5*) and its crystal structure has been solved recently (*6*). The structure reveals that the overall fold and the active site closely resembles that of CCP (*7*). Both proteins have conserved the triad Trp, Arg, and His in the distal pocket, and the triad His, Asp, and Trp in the proximal pocket (Figure 1). Nevertheless, APX forms a porphyrin π cation radical (*8*−*10*) as all the other known peroxidases (*11*−*15*) and not a radical centered on the proximal Trp as CCP (*16*). A potassium ion at about 8 Å from the proximal Trp residue in APX (*8*), and absent in CCP (*7*), may prevent the localization of a cation radical on this Trp residue. Interestingly, the cation-binding site of APX is similar to the proximal Ca^{2+} sites located in peroxidases of both class II and III (*17*−*25*). APX appears to be a better representative member of class I to compare and to probe the structure−function relationship in the "superfamily of plant peroxidases".

In the present work we undertook a detailed analysis of APX in the Fe^{3+} and Fe^{2+} forms and upon ligand binding via electronic absorption and resonance Raman (RR) spectroscopies. Our goal was not only to elucidate the spectral features of APX, but also to ascertain to what degree any property of APX is in common with CCP and/or class II and III peroxidases. Comparison of the data with those obtained previously for bakers' yeast CCP [or recombinant CCPMI and CCPMKT, whose spectroscopy and activity are essentially the same as that of CCP (*26*−*28*)] and other peroxidases allowed us to determine different features in the heme cavity structure of APX with respect to CCP, which instead are shared with peroxidases belonging to class III.

MATERIALS AND METHODS

Recombinant APX has been obtained as previously reported (*5*). Recombinant CCPMI, obtained as described previously (*26*, *27*), has been used in the present work. Since

[†] This work was supported by Italian Consiglio Nazionale delle Ricerche (CNR), Ministero dell'Universita'e Ricerca Scientifica e Tecnologica (MURST), and Cogin. MURST97CFSIB to G.S., U.S. National Science Foundation Grant MCB-0405218 to T.L.P., and Novo Nordisk, Denmark, to M.N.

* To whom correspondence should be addressed. Tel: +39 55 2757596. Fax: +39 55 2476961. E-mail: Smulev@chim.unifi.it.

[‡] Odense University.

[§] Universita' di Firenze.

[||] University of California at Irvine.

[1] Abbreviations: APX, ascorbate peroxidase, ARP, *Arthromyces ramosus* peroxidase; CIP, *Coprinus cinereus* peroxidase expressed in *Aspergillus oryzae*; CCP, cytochrome *c* peroxidase; CCPMI, cytochrome *c* peroxidase expressed in *E. coli* containing Met-Ile at the N-terminus; CCPMKT, cytochrome *c* peroxidase expressed in *E. coli* containing Met-Lys-Thr at the N-terminus; HRP-C, horseradish peroxidase isoenzyme C; RR, resonance Raman; 5-c and 6-c, five-coordinate and six-coordinate hemes; HS, high-spin; LS, low-spin; CT1, long wavelength (>600 nm) porphyrin-to-metal charge-transfer band.

S0006-2960(98)00111-1 CCC: $15.00
Published on Web 05/14/1998

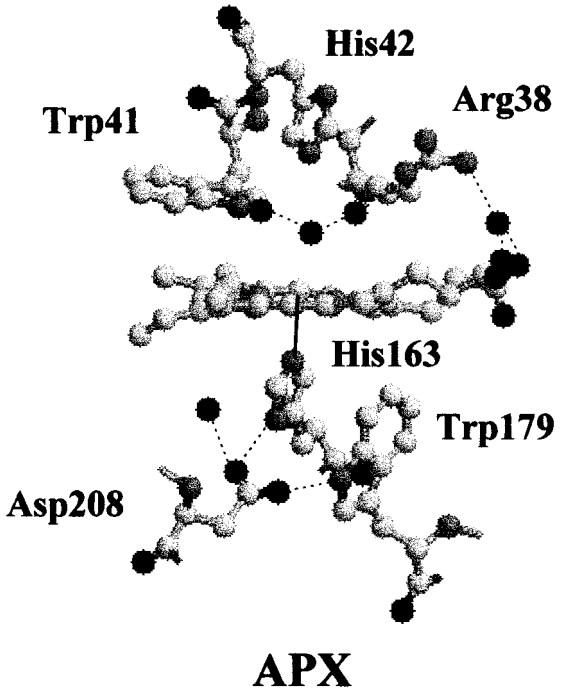

FIGURE 1: Schematic representation of the proximal and distal APX monomer active site. Four ordered water molecules in the cavity are also reported. Dashed lines indicate the inferred H bonds on the basis of distance criteria (*6*).

the spectra of recombinant CCP (either MI or MKT) are essentially unaltered from those of the protein isolated from yeast, we will refer to these peroxidases by the name CCP.

Experiments on Fe^{3+} forms have been carried out in 0.05 and 0.1 M potassium phosphate buffer at pH 7.0 for APX and CCPMI, respectively, and borate buffer, 0.025 M, pH 10.0 (APX). The complexes with sodium fluoride (NaF, Merck) were made by adding NaF (1 M) to the protein solution to give a final concentration of 0.1 M NaF in 0.025 M citric acid-sodium citrate buffer, pH 5.0. The imidazole complex was made by adding imidazole (Merck) to the protein solution (pH 10.0) and following the complexation by the electronic absorption spectrum.

The ferrous forms were prepared by adding a minimum volume of dithionite to deoxygenated buffered solution of protein. The sample in D_2O was prepared by lyophilization of the sample at pH 7.0. The lyophilized material was redissolved in D_2O and the pH adjusted to the final value using NaOD.

Concentrations of the protein were determined spectrophotometrically and were approximately 0.1 mM for resonance Raman and UV−visible absorption spectra.

Absorption spectra were measured with a Cary 5 spectrophotometer. These spectra were measured both prior to and after RR measurements to determine whether sample degradation had occurred. With Soret excitation, the spectra of APX after RR measurements showed an increasing amount of the low-spin species unless very mild conditions were used. In particular, to avoid degradation of the protein upon Soret excitation, 7 mW laser power on the sample and 15 min acquisition were used. To minimize the local heating of the protein induced by the laser beam, the rotating NMR tube was cooled by a gentle flow of N_2 gas passed through liquid N_2. All the RR experiments were collected at about 15° C.

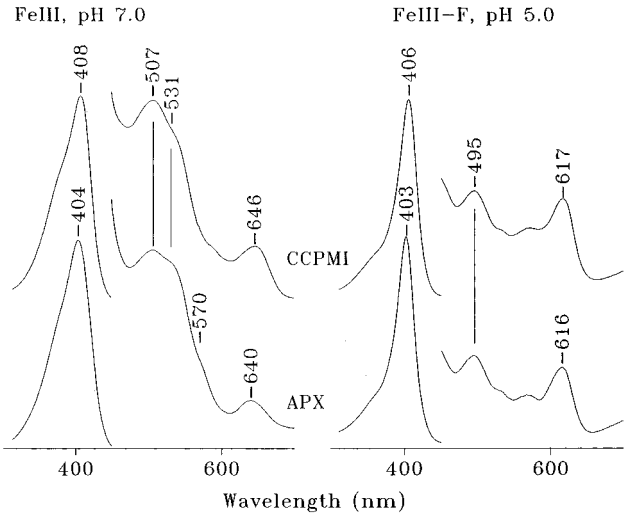

FIGURE 2: Electronic absorption spectra of ferric APX (bottom) and CCP (top) at neutral pH in phosphate buffer (left) and of the corresponding fluoride complexes at pH 5.0 in citrate buffer (right). The region between 450 and 700 nm has been expanded by eight times.

The resonance Raman spectra were obtained by excitation with the 406.7 and 413.1 nm lines of a Kr^+ laser (Coherent Innova 90/K), and the 457.9 and 496.5 nm lines of an Ar^+ laser (Coherent Innova 90/5). The backscattered light from a slowly rotating NMR tube was collected and focused into a computer-controlled double monochromator (Jobin-Yvon HG 2S), equipped with a cooled photomutiplier (RCA C31034 A) and photon-counting electronics. The RR spectra were calibrated to an accuracy of 1 cm^{-1} for intense isolated bands, with indene as a standard.

Experiments at 20 K were performed as previously described (*29*).

Polarized spectra were obtained by inserting a polaroid analyzer between the sample and the entrance slit of the spectrometer. The depolarization ratio, ρ, of the bands at 314 and 460 cm^{-1} of CCl_4 was measured to check the reliability of the polarization measurements using a rotating NMR tube with 180° backscattering geometry. The values obtained, 0.73 and 0.00, compare favorably with the theoretical values of 0.75 and 0.00, respectively.

RESULTS AND DISCUSSION

Figure 2 compares the electronic absorption spectra of recombinant ferric pea cytosolic APX and CCP at pH 7.0 (left) and after addition of fluoride at pH 5.0 (right). For APX at neutral pH as well as at pH 10.0 (data not shown), the Soret band at 404 nm and the visible bands at 507 and 640 nm indicate the presence of high-spin (HS) hemes. Furthermore, the occurrence of the band at 570 nm and the intense shoulder at about 531 nm, as well as the shift of the Soret maximum at 404 nm [1 nm to longer wavelength than in the previously published spectra (*5*, *10*)], are indicative of the presence of a 6-coordinate (6-c) low-spin (LS) species. It is interesting to note that a reasonable amount of a low-spin heme seems to be present also in another recombinant pea cytosolic APX, as judged by the electronic absorption spectrum recently published (*30*). Therefore, the spectrum differs from that of CCP for the blue-shifts of the Soret, despite the presence of a distinct amount of 6-c LS heme,

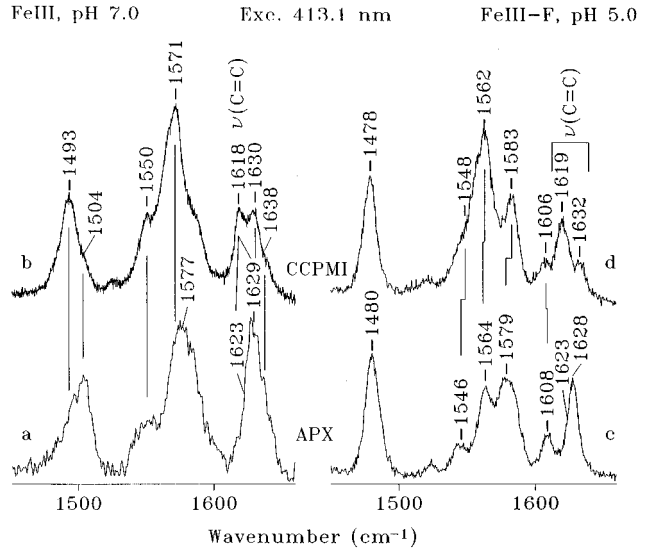

FIGURE 3: Resonance Raman spectra of ferric APX (bottom) and CCP (top) at neutral pH in phosphate buffer (left) and of their F-complexes at pH 5.0 in citrate buffer (right). Experimental conditions: 413.1 nm excitation wavelength, 5 cm^{-1} resolution; (a) 3 s/0.5 cm^{-1} collection interval and 7 mW laser power at the sample; (b) 20 s/0.2 cm^{-1} collection interval and 25 mW laser power at the sample; (c) 8 s/0.5 cm^{-1} collection interval and 20 mW laser power at the sample; (d) 2 s/0.5 cm^{-1} collection interval and 15 mW laser power at the sample.

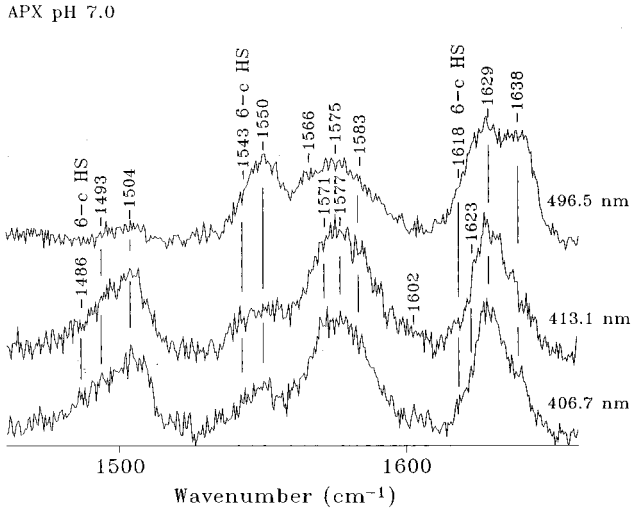

FIGURE 4: Resonance Raman spectra of ferric APX at neutral pH in phosphate buffer 0.05 M taken with different excitation wavelengths. Experimental conditons: 5 cm^{-1} resolution; (406.7 nm) 6 s/0.5 cm^{-1} collection interval and 7 mW laser power at the sample; (413.1 nm) 3 s/0.5 cm^{-1} collection interval and 7 mW laser power at the sample; (496.5 nm) 30 s/0.5 cm^{-1} collection interval and 40 mW laser power at the sample.

and the CT1 bands by 4 and 6 nm, respectively. Addition of fluoride drives both proteins to fully 6-c HS complexes. Nevertheless, the Soret band of the APX-F adduct is blue-shifted by 3 nm with respect to that of CCP-F.

Figure 3 compares the RR spectra, taken with the 413.1 nm laser line, of ferric APX and CCP at pH 7.0 (left) and upon addition of fluoride at pH 5.0 (right). The spectrum of ferric APX appears much more complicated than that of CCP. In fact, three sets of core size marker bands are present, as confirmed by the spectra taken with different excitation wavelengths (Figure 4) and in polarized light (data not shown). These sets correspond to three different species, 5-c HS, 6-c HS, and 6-c LS (*31*), with the 6-c HS form present in a very low amount. It must be noted that APX is particularly unstable in the laser beam. The absorption spectrum of samples irradiated with the 406.7 nm laser line showed an increase of the 6-c LS species, unless very mild conditions were used (see Materials and Methods). Therefore, it cannot be excluded that some 6-c LS heme is formed reversibly during laser irradiation.

The RR spectrum of APX differs also from CCP in the frequency of the ν(C═C) stretching mode. In CCPMI and CCPMKT, the two vinyl substituents give rise to a coincident band at 1618 cm^{-1} (*27*, *32*), whereas in APX, the spectra in polarized light (data not shown) demonstrate the occurrence of two different ν(C═C) stretching modes. A strong polarized RR band at 1629 cm^{-1}, overlapped with the ν_{10} mode of the 5-c HS species, and a weak shoulder at 1623 cm^{-1} occur. The RR spectrum of the APX-F adduct (Figure 3, right) shows only RR bands characteristic of a 6-c HS heme, confirming that the protein fully binds the anion, despite the presence of the 6-c LS heme in the unligated form. The RR spectra of the fluoride complexes of APX vs CCP differ in the frequency of the ν_2 (1564 vs 1562 cm^{-1}), the frequency and relative intensity of the ν_{37} (1579 vs 1583 cm^{-1}), and the relative intensity of the two bands assigned to the vinyl stretching modes. In fact, in the APX-F adduct, the ν(C═C) stretching modes have the same relative intensity as observed in the unligated form, whereas in CCP-F, the vinyl stretch at higher frequency is much weaker than the other band. Indeed, the APX-F spectrum closely resembles the corresponding spectrum of the fluoride complex of horseradish peroxidase isoenzyme C (HRP-C) (*33*).

Upon addition of imidazole, the relative intensity of the vinyl stretching modes changes. The protein becomes a 6-c LS heme species, as shown by the red-shift of the Soret band to 411 nm and the Q-bands at 535 and 559 nm (Figure 5, top) and by the frequency of the RR core size marker bands (Figure 5, bottom). Therefore, the ν_{10} (at 1640 cm^{-1}) no longer overlaps with the vinyl stretches. The RR spectra of the APX−Im complex taken in polarized light in the 1600−1670 cm^{-1} region (Figure 5, bottom) show that the two polarized bands at 1623 and 1632 cm^{-1} have similar intensities.

The assignment of the most intense Raman bands is listed in Table 1 based on the frequencies of heme-model compounds (*31*).

In conclusion, the frequency of the ν(C═C) vinyl stretching modes in the ferric APX is upshifted (1623 and 1629 cm^{-1}) with respect to recombinant CCP where the two vinyl stretches are coincident at 1618 cm^{-1} (*32*). As a consequence, the frequency of the ν_2 mode, being vibrationally coupled with the vinyl stretches (*34*), is also upshifted in APX. The upshift of the vinyl bands in APX indicates weak conjugation of the vinyl double bonds with the heme and this can explain the blue-shift of the Soret absorption maximum of 4 nm compared to CCP, as recently found for the fluoride adducts with various peroxidases (*33*). Changes in vinyl conjugation with the macrocycle π system should result in changes of resonance enhancement of the Raman modes involving these groups when using different excitation wavelengths. This effect has been recently observed in the deoxy form of hemoglobin from *Chelidonichthys kumu*

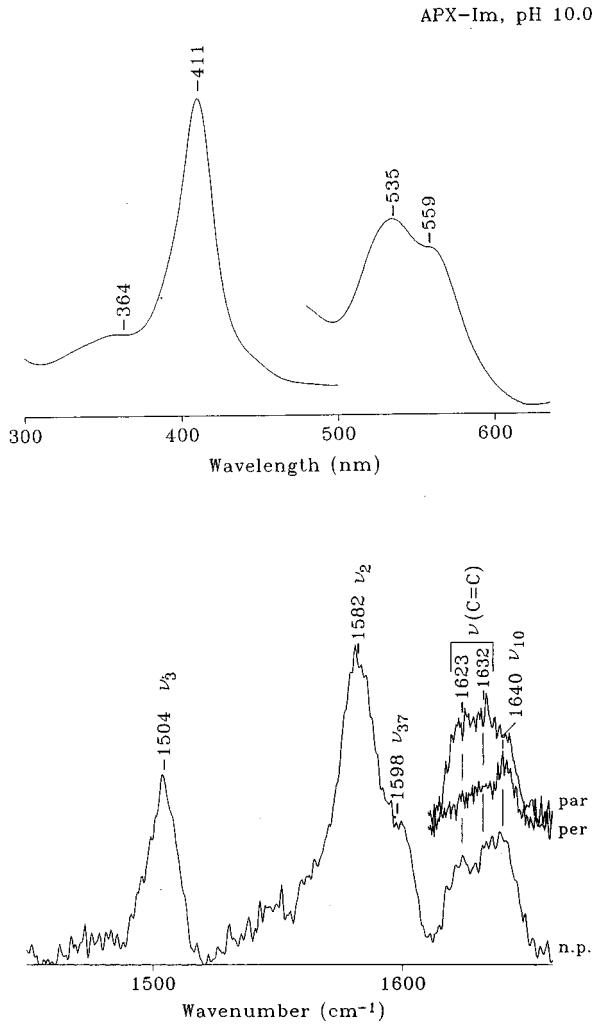

FIGURE 5: APX−Im complex at pH 10.0. (Top) Electronic absorption spectrum. The region between 450 and 700 nm has been expanded by eight times. (Bottom) RR spectra in the 1450−1700 cm^{-1} region obtained with the 413.1 nm excitation. The measurements made in polarized light are shown in the 1600−1700 cm^{-1} region. Experimental conditions: 5 cm^{-1} resolution; 25 mW laser power at the sample; (nonpolarized, n.p.) 17 s/0.5 cm^{-1} collection interval; (parallel, par) 25 s/0.5 cm^{-1} collection interval; (perpendicular, per) 19 s/0.5 cm^{-1} collection interval.

(Smulevich, G., Possenti, M., D′Avino, R., Di Prisco, G., and Coletta, M. unpublished data). In the present case, the overlapping of three different ν_{10} modes in the vinyl region together with the extremely weakness of one ν(C═C) (Figure 3) makes it difficult to evaluate the intensity changes between the two vinyl stretches.

Interestingly, the formation of the imidazole complex causes a change in the conjugation of at least one vinyl double bond as indicated by the upshift of one vinyl stretch to 1632 cm^{-1}. A similar effect has been observed previously in the Im-adduct of a mutant of *Coprinus cinereus* peroxidase (CIP), whose distal Phe54 has been replaced by Trp (Neri, F., Baldi, B., Welinder, K. G., and Smulevich, G., unpublished data), and for CCP at alkaline pH where a protein conformational change that specifically involves the 2-vinyl substituent occurs with the concomitant binding of the distal His to the heme iron (*32*).

The electronic absorption spectrum of APX in the ferrous form is in agreement with the earlier published spectrum (*4*). The electronic absorption and the RR (Figure 6 and Table 1) spectra are characteristic of 5-c HS heme at both pH 7.0 and 10.0 (data not shown). An overall blue-shift by 3−4 nm is observed in the electronic absorption spectrum as compared to that of CCP (*35*). On the other hand, the RR spectrum of ferrous APX in the high-frequency region differs from that of CCP (*36*) mainly in the frequencies of the ν_2 (1561 vs 1564 cm^{-1}), the ν_{37} (1582 vs 1584 cm^{-1}), and the ν(C═C) stretching modes (1624 vs 1617 cm^{-1}). The vinyl stretching modes are shifted to higher frequency compared to CCP (*32*, *36*), as observed for the ferric forms. Therefore, the 7 cm^{-1} upshift of the vinyl stretches is consistent with the 4 nm blue-shift of the electronic absorption spectrum as compared to the CCP spectrum (*36*).

In the low-frequency region, the 5-c HS ferrous heme proteins are characterized by a strong band in the 200−250 cm^{-1} region assigned to the ν(Fe−Im) stretching mode on the basis of the isotopic shift observed in ^{54}Fe-reconstituted proteins *(37)*. Among the various hemoproteins, peroxidases are characterized by an Fe−Im stretch at relatively high frequency, due to the strong hydrogen bond between the N_δ atom of the imidazole fifth ligand and the oxygen atom of the aspartic acid side chain (Figure 1), which imparts an imidazolate character to the ligand. Another consequence of the hydrogen bond is the frequency shift observed at alkaline pH and in deuterated buffer (*27*, *38*).

Figure 7 compares the RR spectra of ferrous APX taken in buffer, pH 10.0 (bottom) and pH 7.0 (middle), and deuterated buffer, pD 7.5 (top). The spectra markedly differ from those of CCP in both the frequencies and intensities of the bands (*32*). In particular, the band at 405 cm^{-1} appears extremely weak and broad. This band is assigned to the $\delta(C_\beta C_a C_b)$ bending mode of the vinyl substituents, by analogy with the intense band observed at 402 cm^{-1} in CCP (*32*). The intensity decrease and the broadening observed in APX suggest a slightly different frequency of the two $\delta(C_\beta C_a C_b)$ bending modes, corresponding to the observed splitting of the ν(C═C) stretching modes in the high-frequency region. A similar behavior has been observed for CCP at alkaline pH where a distinct upshift and broadening of the vinyl bands were observed (*32*).

In the region of the ν(Fe−Im) stretching mode, three bands appear to be sensitive to deuteration or alkaline pH. The strong band at 234 cm^{-1}, insensitive to the D_2O isotopic substitution, but downshifting by 2 cm^{-1} at pH 10.0, the weak band at 207 cm^{-1} which downshifts to 204 cm^{-1} in both D_2O and alkaline pH, and the band at 261 cm^{-1} which downshifts to 258 cm^{-1} in D_2O. In agreement with the similar results obtained recently for ferrous CCP (*32*), we assign the bands at 234 and 207 cm^{-1} to two ν(Fe−Im) stretching modes. The two ν(Fe−Im) stretching modes at 233 and 246 cm^{-1} in CCP have been explained as arising from two tautomers of the hydrogen bond between the His175 imidazole and the Asp235 carboxylate side chain. In one tautomer, the proton resides on the imidazole (lower frequency) while in the other the proton is transferred to the carboxylate. At alkaline pH, only the 233 cm^{-1} band is present in CCP (32). On the other hand, the absence of a decrease of the I_{234}/I_{207} intensity ratio between the two bands of APX at alkaline pH suggests that the two species are independent and not in equilibrium as in CCP or CIP. The frequencies are lower in APX (207 and 234 cm^{-1}) as compared to CCP in agreement with the crystal structures.

Table 1: Mode Assignment and Frequencies of the Principal RR Bands (cm^{-1}) Observed for Ferric and Ferrous APX

	Fe^{3+}					
mode	6-c HS (F^-)	5-c HS	6-c LS	6-c LS (Im^-)	LT, 6-c LS	Fe^{2+}, 5-c HS
ν(C=C)	1628, 1623	1629, 1623		1632, 1623	1633, 1628	1624
ν_{10}	1608	1629	1638	1640	1646	1603
ν_{37}	1579	1583	1602	1598	1607	1582
ν_{19}		1575				
ν_2	1564	1571	1577	1582	1587	1561
ν_{11}	1546	1550	1566	1562	1572	1547
ν_3	1480	1493	1504	1504	1512	1470
ν_4	1373	1375		1375	1377	1356
$\delta(C_\beta C_a C_b)$						405
$\delta(C_\beta C_c C_d)$						370
ν_8						346
γ_6						314
ν(Fe−Im)						234, 207

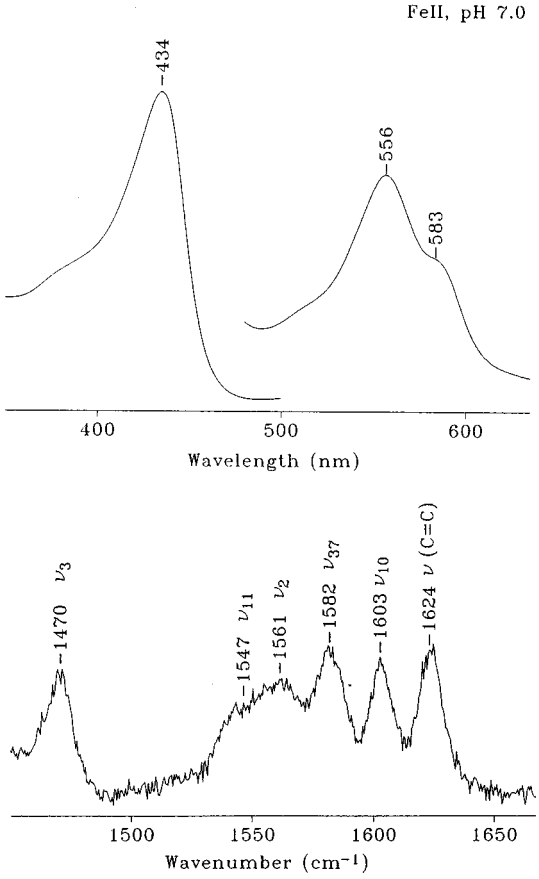

FIGURE 6: Ferrous APX at neutral pH in phosphate buffer. (Top) Electronic absorption spectrum. The region between 450 and 700 nm has been expanded by 5 times. (Bottom) RR spectrum in the 1450−1700 cm^{-1} region. Experimental conditions: 457.9 nm excitation wavelength, 5 cm^{-1} resolution; 9 s/0.5 cm^{-1} collection interval and 25 mW laser power at the sample.

In fact, in APX, the Fe−His163 and the His163−Asp208 distances are 2.15 and 3.2 Å, respectively (*6*), whereas in CCP the corresponding values are shorter (2.0 and 3.0 Å, respectively) (*6*, *7*). While these differences are close to the limits detectable at the resolution of the various crystal structures, the trend correlates well with our present results. One of the ν(Fe−Im) stretching modes (207 cm^{-1}) and the 261 cm^{-1} band revealed a D_2O effect (Figure 7), the modes shifting to 204 and 258 cm^{-1}, respectively. These effects previously observed in CCP and in its Trp191Gln and Trp191Gly mutants indicate that only the Fe−His stretch corresponding to the proton residing on the imidazole shifts

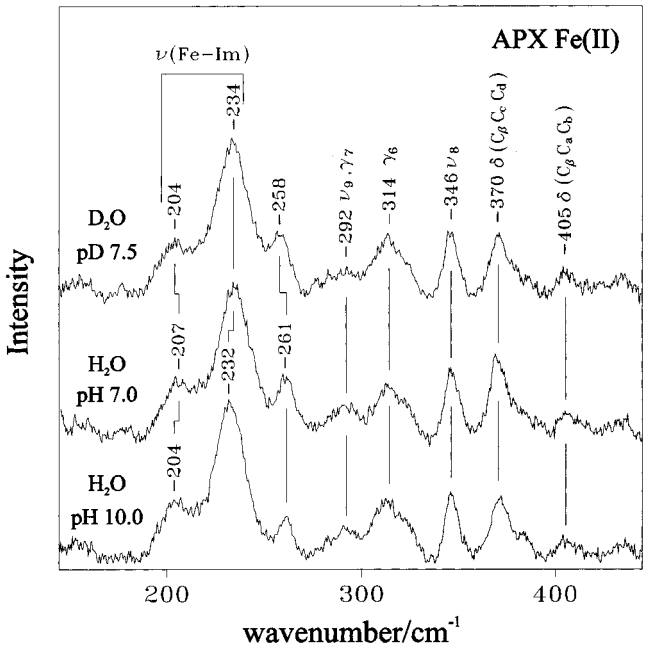

FIGURE 7: RR spectra of ferrous APX in the low-frequency region in H_2O (pH 7.0) and D_2O (pD 7.5) phosphate buffer 0.05 M and borate buffer 0.025 M, pH 10.0. Experimental conditions: 457.9 nm excitation wavelength, 5 cm^{-1} resolution, 25 mW laser power at the sample; (H_2O, pH 10.0) 12 s/0.5 cm^{-1} collection interval; (H_2O, pH 7.0) 10 s/0.5 cm^{-1} collection interval; (D_2O, pD 7.5) 12 s/0.5 cm^{-1} collection interval.

upon D_2O substitution. Interestingly, the frequency of the band at 207 cm^{-1} of APX closely resembles that observed for the Asp235Asn CCP mutant (205 cm^{-1}). This low frequency has been attributed to the loss of the His175−Asp235 H bond, and no isotopic sensitivity in D_2O has been observed (32). The D_2O sensitivity of the 261 cm^{-1} band of APX suggests its assignment to a histidine mode (*32*). This band has so far only been identified in ferrous APX, CCP, and CIP (*36*). Its enhancement in these cases result from coupling to the Fe−His stretch, as revealed by its disappearance when the latter is shifted out of the region [as in the Asp235Asn CCP mutant (*32*)].

Comparison between CCP and APX. APX shares many common characteristics with CCP, although some differences have been pointed out in the above results and discussion section.

Similarities. (1) From the electronic absorption spectra and, in particular, from the wavelength of the CT1 band, it

can be concluded that APX binds fluoride in the same way as CCP. In fact, it has been found recently that the wavelength of the CT1 band is a sensitive probe of axial ligand polarity and of its interactions with the distal protein residues. In particular, if the ligand acts as a hydrogen-bond acceptor, then the greater the number and strength of the hydrogen bonds, the longer the wavelength of the CT1 band. Therefore, the wavelength of the CT1 band at 616 nm, analogous with recent observations for CCP, but 4−6 nm red-shifted with respect to peroxidases of class II and III, indicates that the fluoride anion, bound to the Fe atom, is stabilized by three hydrogen bonds; probably with Arg38, a water molecule bridged with the distal His, and Trp41. The distal Trp is conserved only in class I peroxidases, while in classes II and III, it is substituted by a phenylalanine residue (*1*). Therefore, for the peroxidases of classes II and III, the fluoride ligand is stabilized by only two hydrogen bonds, as suggested by the blue-shift of the CT1 band compared to CCP (*33*).

(2) The presence of a very broad RR band in the region of the Fe−Im stretching mode can be due to the coexistence of two separate bands arising from the stretching of the bond between the Fe atom and the proximal histidine ligand. These two bands differ for the hydrogen-bond strength between the N_δ atom of the His163 and the Asp208 carboxylate side chain. The RR frequencies confirm the proposal that the His-Asp hydrogen bond is weaker in APX than in CCP, in agreement with the longer hydrogen-bond distance for the Asp208−His163 vs the Asp235−His175 [3.2 Å in APX vs 3.0 Å in CCP (*6*, *7*)].

The finding of two separate bands arising from the Fe−Im stretch is in common also with CIP, which belongs to class II, but differs markedly from all peroxidases of class III so far investigated which are characterized by a single sharp band (*39*).

Differences. (1) The presence in ferric APX of a discrete amount of a 6-c LS heme coexisting with the 5-c HS and the minor 6-c HS species was not revealed in the native protein (*5*).

It is known that the properties and stability of APX vary considerably depending on the source of the enzyme, with the Soret band maximum varying from 403 to 407 nm (*40*). The crystal structure of APX reveals the presence of a water molecule sitting above the Fe atom at about 2.7 Å and, therefore, not bound to the iron. Such a distance is not necessarily maintained in solution, and differences in the spin and coordination states of peroxidases between solution and single crystal have been reported already. For example, manganese peroxidase, whose crystal structure shows a 5-c HS heme with a water molecule at 2.7 Å from the iron atom (*22*), is a mixture of 5- and 6-c HS heme, with the latter being predominant, in solution, as indicated by the RR experiments (*41*). Another interesting case is represented by the Arg48Lys CCPMI mutant, which is 5-c HS in its crystal form (*42*) and mainly 6-c LS heme in solution (*27*, *42*). Therefore, it is not surprising that the Fe atom of APX has the sixth position occupied by a ligand which might be simply a water molecule with some OH^- character (i.e. strongly hydrogen bonded), as previously observed for the Asp235Asn CCP mutant (*27*) and not an internal strong-field ligand such as the distal His, as observed for CCP at alkaline pH (*43*, *44*). This is suggested by the spectral differences observed for the low-spin species in the electronic spectra of the ferric form and the Im complex, namely the α-band around 570 nm in the ferric form, vs 559 nm in the Im-complex. In fact, it has been shown that the Im−Fe-OH complexes are characterized by distinctly red-shifted $\alpha-\beta$ bands relative to those of the Im−Fe-Im adducts (*43*). In accord with the interpretation on the nature of the sixth ligand of ferric APX, fluoride is able to displace the low-spin ligand giving rise to a complete 6-c HS heme. Therefore, the formation of the low-spin heme either during the preparation or during the Raman experiment can simply be due to a slight change of the location and/or orientation of the distal residues which are hydrogen-bonded with water molecules (i.e., Trp, His, and Arg) (Figure 1). Actually, the same effect in the laser beam has been observed for CIP at neutral pH (*36*), and comparing the X-ray structures of CCP (*7*), APX (*6*), and *Arthromyces ramosus* peroxidase (ARP) (*19*, *20*), which is the same as CIP (*21*), we noticed that in APX and ARP/CIP the guanidinium group of the distal Arg is located at a longer distance (about 1 and 0.5 Å, respectively) from the heme iron than in CCP. As a consequence, the hydrogen bond between the N_ϵ of the distal Arg (Arg38 for APX and Arg51 for CIP) and the water molecule bridged to the water molecule sitting above the Fe atom is about 0.5 Å longer than in CCP.

Experiments at low temperature (20 K) (Table 1, LT) appear to confirm a different behavior between CCP and APX. In fact, at 20 K, APX was found to be almost exclusively 6-c LS as previously found for CCP (*45*, *46*), and in agreement with the results obtained with EPR spectroscopy (*8*). But in contrast with CCP (*43*), glycerol did not prevent the formation of the 6-c LS in ferric APX at 20 K. Moreover, the RR frequencies (data not shown) of ferrric APX at 20 K are very similar to those reported for alkaline HRP-C (*29*), with an overall upshift by 7−10 cm^{-1} of the core size marker bands with respect to room temperature (Table 1) and two ν(C═C) stretching modes at 1628 and 1633 cm^{-1}.

(2) Two distinct vinyl stretching modes are observed in all the Fe^{3+} forms of APX under investigation, as for peroxidases of class III so far studied (*39*, *47*). Ferric CCP at neutral pH has both vinyl stretches coincident at 1620 cm^{-1} (*48*) [at 1618 cm^{-1} for recombinant CCP (*27*, 32)], two resolved vinyl modes in the 6-c LS form at alkaline pH [where the band due to the vinyl in position 2 moved to 1628 cm^{-1} (*32*)], and two resolved bands due to vinyls in the fluoride complex (*33*).

Analysis of the X-ray structures of the peroxidases so far solved indicate that the orientation of the vinyl groups are rather different, especially for the vinyl in position 2. Actually, the vinyl 2 dihedral angle varies widely, whereas vinyl 4 is characterized by values varying in a smaller range. Accordingly, the RR vinyl C═C stretches of peroxidases vary from about 1618 to 1631 cm^{-1}. The higher the frequency of the vinyl stretch, the less conjugated is its double bond with the porphyrin macrocycle resulting in a blue-shift of the $\pi \rightarrow \pi^*$ transitions in the electronic absorption spectrum (*33*). Linear relationships between the ν(C═C) stretching mode frequencies and the angle ϕ (i.e., the angle between the projections of the vinyl and pyrrole C═C double bonds on the heme mean plane) as well as the torsion angle τ have been found (*49*).

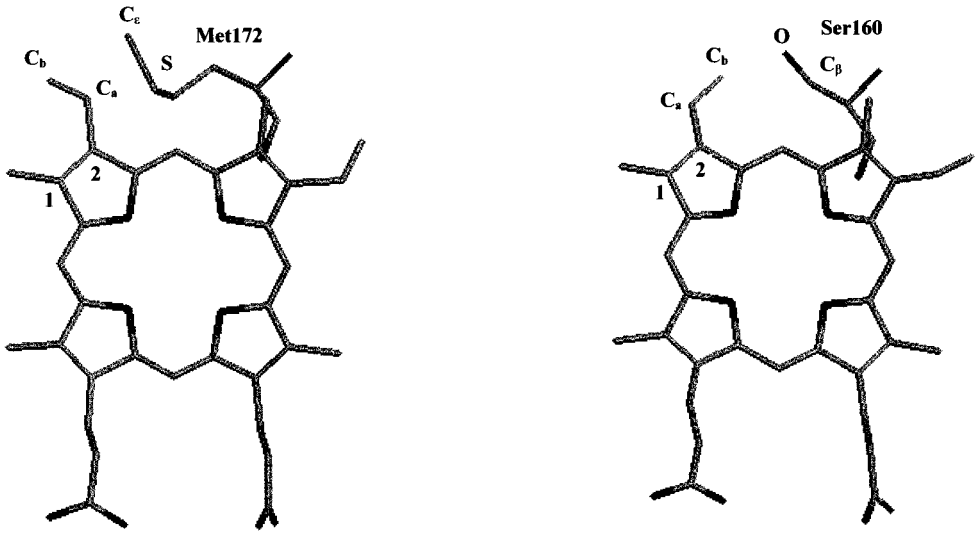

	Met172		Ser160	
	C_ε	S	O	C_β
C_2	5.0	4.2	6.0	6.6
C_a	4.1	3.8	5.3	6.2
C_b	4.0	4.1	4.0	5.0

FIGURE 8: Representation of the steric hindrance between the vinyl 2 of the heme and Met172 (CCPMI) (*52*) and Ser160 (APX) (6). The inserted table reports the measured distances (Å).

Recently, based on the RR spectra and local density functional calculations on mono- and divinylhemins, it has been proposed that when the protein matrix exerts no constraints on the vinyl groups of heme proteins, two distinct ν(C═C) stretching modes should be observed in their RR spectrum. Furthermore, the calculations suggested the appearance of the two ν(C═C) stretches at about 1620 and 1630 cm^{-1}. The first band is assigned to a nearly in-plane vinyl group pointing toward the β-pyrrole methyl group, the other to an out-of-plane vinyl group pointing toward the meso-hydrogen of the heme (*50*). Considering that the dihedral angles for CCPMI are $\tau = 152.1°$ and 156.5° ($\phi =$ 6° and 2°) for vinyl 2 and 4, respectively, whereas for APX, $\tau = 27.5°$ ($\phi = 64°$) and 125.1° ($\phi = 19°$) (mean angles over the four asymmetric units of the crystal derived from the values $\tau = 19.5°$, 40.9°, 15.3°, and 34.2° and $\tau = 116.2°$, 137.3°, 123.6°, and 123.2° for vinyl 2 and 4, respectively), we assigned the band at 1623 cm^{-1} of APX to the vinyl substituent in position 4, and the band at 1629 cm^{-1} to the vinyl in position 2. By a combined inspection of the CCP and APX structures it appears that the very different orientation of the vinyl 2, and therefore the very different RR frequency, is due to the steric hindrance exerted by the protein matrix on the vinyl. In CCP, the Met172 side chain is found in the close proximity to the vinyl 2, whereas in APX this residue is the less encumbered serine (Ser160). Figure 8 shows the hemes of CCPMI and APX with the residue in the close proximity of vinyl 2. The inserted table reports the distances between the atoms of the side chain and the carbon atoms C_2, C_a, and C_b of the vinyl group. It can be seen that the C_a and C_2 atoms are much farther from the oxygen and the C_β atoms of Ser160 (APX) than from the C_ϵ and S atoms of Met172 (CCP). It is interesting to note that the same Ser residue is also found in the close proximity of the vinyl 2 of HRP-C and barley peroxidase, both belonging to class III (*1*) (Welinder 1992), for which two vinyl RR bands, at a frequency similar to those observed for APX, were found (*39*, *47*).

From the analysis of sequence data available for all plant ascorbate peroxidases, seven distinct types of ascorbate peroxidases have been found. Two types of cytosolic soluble, three types of cytosolic membrane-bound (predicted), and two types of chloroplast APX, one soluble and one membrane-bound, have been reported (*51*). It is interesting to note that some of those are monomeric and that two types have both the proximal and distal Trp residues substituted by Phe residues. All the other key residues in the active site, the proximal cation-binding site and the serine residue in the proximity of the vinyl 2 group, are conserved. Therefore, it appears that ascorbate peroxidases provide the first clear example in which it can be shown that the protein matrix plays a role in directing the orientation of the vinyl groups of the heme chromophore. The fact that both vinyl groups are largely unconstrained by the protein matrix allows them to assume the preferred conformation characterized by two distinct RR ν(C═C) stretching modes. Their RR frequencies and the overall blue-shift of the electronic absorption spectrum maxima indicate that only one vinyl group is mainly conjugated with the double bonds of the heme group. For several heme proteins, it has been suggested that the vinyl double bond may provide a conduit for electronic communication between the porphyrin macrocycle and the protein matrix (*50*). Therefore, the fact that in APX peroxidases the residue that governs the protein−vinyl 2 interaction is invariant may indicate that the vinyl orientation is important to peroxidase activity. Further work,

however, is necessary before any firm conclusions can be drawn regarding the role of vinyl conjugation in heme proteins.

REFERENCES

1. Welinder, K. G. (1992) *Curr. Opin. Struct. Biol. 2*, 383−393.
2. Mittler, R., and Zilinskas, B. A. (1991) *FEBS Lett. 289*, 257−259.
3. Welinder, K. G., and Gajhede, M. (1993) in *Plant Peroxidases: Biochemistry and Physiology* (Welinder, K. G., Rasmussen, S. K., Penel, C., and Greppin, H., Eds.) pp 35−42, University of Geneva, Geneva.
4. Mittler, R., and Zilinskas, B. A. (1991) *Plant Physiol. 97*, 962−968.
5. Patterson, W. R., and Poulos, T. L. (1994) *J. Biol. Chem. 269*, 17020−17024.
6. Patterson, W. R., and Poulos, T. L. (1995) *Biochemistry 34*, 4331−4341.
7. Finzel, B. C., Poulos, T. L., and Kraut, J. (1984) *J. Biol. Chem. 259*, 13027−13036.
8. Patterson, W. R., Poulos, T. L., and Goodin, D. B. (1995) *Biochemistry 34*, 4342−4345.
9. Pappa, H., Patterson, W. R., and Poulos, T. L. (1996) *J. Biol. Inorg. Chem. 1*, 61−66.
10. Marquez, L. A., Quitoriano, M., Zilinskas, B. A., and Dunford, H. B. (1996) *FEBS Lett. 389*, 153−156.
11. Dolphin, D., Forman, A., Borg, D. C., Fajer, J., and Felton, R. H. (1971) *Proc. Natl. Acad. Sci. U.S.A. 68*, 614−618.
12. Andrawis, A., Johnson, K. A., and Tien, M. (1988) *J. Biol. Chem. 263*, 1195−1198.
13. Wariishi, H., Akileswaran, L., and Gold, M. H. (1988) *Biochemistry 27*, 5365−5370.
14. Andersen, M. B., Hsuanyu, Y., Welinder, K. G., Schneider, P., and Dunford, H. B. (1991) *Acta Chem. Scand. 45*, 1080−1086.
15. Farhangrazi, Z. S., Copeland, B. R., Nakayama, T., Amachi, T., Yamazaki, I., and Powers, L. S. (1994) *Biochemistry 33*, 5647−5662.
16. Sivaraja, M., Goodin, D. B., Smith, M., and Hoffman, B. M. (1989) *Science 245*, 738−740.
17. Poulos, T. L., Edwards, S. L., Wariishi, H., and Gold, M. H. (1993) *J. Biol. Chem. 268*, 4429−4440.
18. Piontek, K., Glumoff, T., and Winterhalter, K. (1993) *FEBS Lett. 315*, 119−124.
19. Kunishima, N., Fukuyama, K., Matsubara, H., Hatanaka, H., Shibano, Y., and Amachi, T. (1994) *J. Mol. Biol. 235*, 331−344.
20. Kunishima, N., Amada, F., Fukuyama, K., Kawamoto, M., Matsunaga, T., and Matsubara, H. (1996) *FEBS Lett. 378*, 291−294.
21. Petersen, J. F. W., Kadziola, A., and Larsen, S. (1994) *FEBS Lett. 339*, 291−296.
22. Sundaramoorthy, M., Kishi, K., Gold, M. H., and Poulos, T. L. (1994) *J. Biol. Chem. 269*, 32759−32767.
23. Schuller, D. J., Ban, D. N., van Huystee, R. B., McPherson, A., and Poulos, T. L. (1996) *Structure 4*, 311−321.
24. Gajhede, M., Schuller, D. J., Henriksen, A., Smith, A. T., and Poulos, T. L. (1997) *Nat. Struct. Biol. 4*, 1032−1038.
25. Henriksen, A., Welinder, K. G., and Gajhede, M. (1998) *J. Biol. Chem. 273*, 2241−2248.
26. Fishel, B. C., Villafranca, J. E., Mauro, J. M., and Kraut, J. (1987) *Biochemistry 26*, 351−360.
27. Smulevich, G., Mauro, J. M., Fishel, L. A., English, A. M., Kraut, J., and Spiro, T. G. (1988) *Biochemistry 27*, 5477−5485.
28. Houseman, A. L. P., Doan, P. E., Goodin, D. B., and Hoffman, B. M. (1993) *Biochemistry 32*, 4430−4443.
29. Feis, A., Marzocchi, M. P., Paoli, M., and Smulevich, G. (1994) *Biochemistry 33*, 4577−4583.
30. Hill, A. P., Modi, S., Sutclippe, M. J., Turner, D. D., Gilfoyle, D. J., Smith, A. T., Tam, B. M., and Lloyd, E. (1997) *Eur. J. Biochem. 248*, 347−354.
31. Choi, S., Spiro, T. G., Langry, K. C., Smith, K. M., Budd, D. L., and La Mar, G. N. (1982) *J. Am. Chem. Soc. 104*, 4345−4351.
32. Smulevich, G., Hu, S., Rodgers, K. R., Goodin, D. B., Smith, K. M., and Spiro, T. G. (1996) *Biospectroscopy 2*, 365−376.
33. Neri, F., Kok, D. Miller, M. A., and Smulevich, G. (1997) *Biochemistry 36*, 8947−8953.
34. Spiro, T. G., and Li, X.-Y (1988) in *Biological Applications of Raman Spectroscopy*, Vol. III (Spiro, T. G., Ed.) pp 1−37, John Wiley & Sons, New York.
35. Conroy, C. W., Tyma, P., Daum, P. H., and Erman, J. E. (1978) *Biochim. Biophys. Acta 537*, 62−69.
36. Smulevich, G., Feis, A., Focardi, C., Tams, J., and Welinder K. G. (1994) *Biochemistry 33*, 15425−15432.
37. Kitagawa, T. (1988) in *Biological Applications of Raman Spectroscopy*, Vol. III (Spiro, T. G., Ed.) pp 97−131, John Wiley and Sons, New York.
38. Teraoka, J., and Kitagawa, T. (1981) *J. Biol. Chem. 256*, 3969−3977.
39. Smulevich, G. (1996) in *Plant Peroxidases: Biochemistry and Physiology* (Obinger, C., Burner, U., Ebermann, R., Penel, C., and Greppin, H., Eds.) pp 13−19, University of Geneva, Geneva.
40. Dalton, D. A. (1991) in *Peroxidases in Chemistry and Biology*, Vol. II, (Everse, J., Everse, K. E., and Grisham, M. B., Eds.) pp 139−153, CRD Press, Boca Raton, FL.
41. Kishi, K., Kusters-van Someren, M., Mayfield, M. B., Loehr, T. M., and Gold, M. H. (1996) *Biochemistry 35*, 8986−8994.
42. Vitello, L. B., Erman, J. E., Miller, M. A., Wang, J., and Kraut, J. (1993) *Biochemistry 32*, 9807−9818.
43. Smulevich, G., Miller, M. A., Kraut, J., and Spiro, T. G. (1991) *Biochemistry 30*, 9546−9558.
44. Turano, P., Ferrer, J. C., Cheesman, M. R., Thompson, A. J., Banci, L., Bertini, I., and Mauk, A. G. (1995) *Biochemistry 34*, 13895−13905.
45. Yonetani, T., and Anni, H. (1987) *J. Biol. Chem. 262*, 9547−9554.
46. Smulevich, G., Mantini, A. R., English, A. M., and Mauro, J. M. (1989) *Biochemistry 28*, 5058−5064.
47. Smulevich, G., Paoli, M., Burke, J. F., Sanders, S. A., Thorneley, R. N. F., and Smith, A. T. (1994) *Biochemistry 33*, 7398−7407.
48. Smulevich, G., Wang, Y., Edwards, S. L., Poulos, T. L., English, A. M., and Spiro, T. G. (1990) *Biochemistry 29*, 2586−2592.
49. Smulevich, G., Neri, F, and Marzocchi, M. P. (1997) in *Spectroscopy of biological molecules: modern trends* (Carmona, P., Navarro, R., and Hernanz, A., Eds.) pp 85−86, Kluwer Academic Publishers, Dordrecht, The Netherlands.
50. Kalsbeck, W. A., Ghosh, A., Pandey, R. K., Smith, K. M., and Bocian, D. F. (1995) *J. Am. Chem. Soc. 117*, 10959−10968.
51. Jespersen, H. M., Kjærsgård, I. V. H., Østergaard, L., and Welinder, K. G. (1997) *Biochem. J. 326*, 305−310.
52. Wang, J., Mauro, J. M., Edwards, S. L., Oatley, S. L., Fishel, L. A., Ashford, V. A., Xuong, N.-h., and Kraut, J. (1990) *Biochemistry 29*, 7160−7173.

BI980111Z